Improving tumour ADC estimates and elucidating tumour heterogeneity using adaptive Bayesian Markov random field Monte Carlo

S. Walker-Samuel[1], M. Orton[1], J. K. Boult[1], and S. P. Robinson[1]
[1]Cancer Research UK & EPSRC Cancer Imaging Centre, The Institute of Cancer Research, Sutton, Surrey, United Kingdom

Introduction: The spatial distribution of apparent diffusion coefficient (ADC) estimates in tumours is typically heterogeneous, although decoupling the contribution of measurement uncertainty and true regional variation is challenging. In this study, the use of an adaptive Bayesian Markov random field model to estimate ADC values was evaluated and applied *in vivo*. This approach has previously shown promise in reducing the uncertainty associated with parameter estimates in dynamic contrast-enhanced MRI [1], by using neighbouring pixels to inform the fit to a set of data from a given voxel. Furthermore, the 'borrowing strength' assigned to each pixel can be used to create a map of tumour regions with similar ADC estimates, thereby elucidating tumour heterogeneity. In this study, the feasibility of using adaptive smoothing to estimate tumour ADC values was evaluated and the uncertainty and accuracy of ADC estimates compared with the standard approach in which voxels are treated as independent.

Materials and Methods: *Statistical Model:* A Markov chain Monte Carlo (MCMC) approach was used to construct probability density functions on a pixel-by-pixel basis, using a hierarchical Bayesian model. Within this, the data model assumed Rice-distributed magnitude MR data, which has recently been shown to provide good ADC accuracy in tumours compared with other approaches [2,3]. A single exponential decay was used for the process model:

$$S(b \mid \alpha, \beta) = \exp(\alpha)\exp\left(-b\exp(\beta)\right) \equiv S_0 \exp\left(-bADC\right)$$

where α and β are fitted parameters ($\exp(\alpha)=S_0$ and $\exp(\beta) = ADC$). A Gibbs sampler with Metropolis-Hastings updates was used for the Markov chain Monte Carlo (MCMC) analysis, in which random samples from the joint posterior of α and β were obtained. Histograms are constructed for each parameter from the trajectory of their random walk, from which the expectation value and spread determine a point estimate and uncertainty, respectively. As per Schmid *et al* [1], the differences in the values of α and β in neighbouring voxels were assumed to be Gauss-distributed. The precision (inverse of the variance) of these distributions defines the strength of the smoothing between neighbouring pixels and these precision parameters were included in the Bayesian model and estimated using Gibbs sampling; a large estimated precision implies strong borrowing from a neighbour, whilst a small precision implies weak borrowing.

Simulation: A 20×20 matrix *ADC* map was generated with central and peripheral circular regions with differing (uniform) values to represent a typical tumour distribution with viable tumour rim ($ADC_{rim}=1\times10^{-3}$ mm^2/s) and central necrotic region ($ADC_{core}=3\times10^{-3}$ mm^2/s). Simulated acquisition parameters mirrored those used *in vivo* and a signal-to-noise ratio for the first b-value data point was set equal to 10. The relative accuracy and precision of ADC estimates with and without the Markov random field were evaluated.

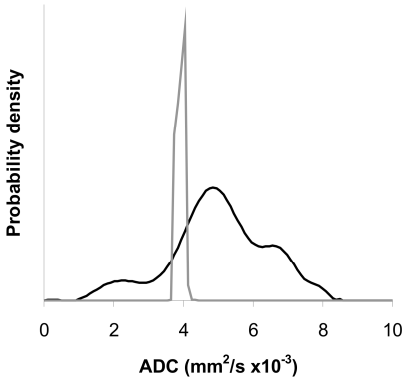

Figure 1: ADC probability density functions for simulated diffusion data (ADC=0.004mm^2/s) without (black line) and with (grey line) adaptive smoothing.

In Vivo: ADC point estimates and uncertainties were measured in two mouse tumour models: a subcutaneous C6 glioma (n=5) and orthotopic PC3 prostate tumours (n=5). Acquisition parameters included: 6 b-values (6, 41, 109, 210, 337 and 504 s/mm^2, TR=1000ms, TE=36 ms, field of view=3×3cm, slice thickness=1mm, matrix size=128×128.

Results: Figures 1 and 2 show example ADC probability density functions and ADC point estimate and uncertainty maps, respectively, both with and without adaptive smoothing. It is clear that use of the adaptive Markov random field reduces scatter in the point estimate maps and significantly reduces the associated uncertainty. In simulations, the adaptive Markov random field significantly reduced the relative error in ADC estimates from (13.3±5.4)% to (4.8±3.1)% ($p<0.001$) and the relative uncertainty from (17.4±5.0)% to (0.46±0.92)% ($p<0.001$). Inspection of the spatial distribution of precision (smoothing) parameters shows clear delineation between the two tumour regions and the background noise (Figure 2d and h). *In vivo*, the absolute uncertainty in ADC estimates was significantly reduced from $(0.12\pm0.08)\times10^{-3}$ mm^2/s to $(0.009\pm0.01)\times10^{-3}$ mm^2/s ($p<0.001$), corresponding to an average 81.2% improvement in precision. Visual inspection of the distribution of spatial components within tumour ROIs revealed much greater heterogeneity in PC3 orthotopic prostate tumours compared with C6 subcutaneous tumours.

Discussion and Conclusion: The precision and accuracy of ADC estimates in tumours was significantly improved by use of Bayesian adaptive Markov random field model, compared with an equivalent model without adaptive smoothing. This approach is promising as it allows ADC estimates to be greatly improved without changing acquisition parameters. Thus, high resolution data or fewer averages could be acquired for the same estimate precision. Furthermore, elucidation of homogeneous regions of tumour tissue may help inform tumour tissue classification by reducing the confounding influence of measurement imprecision.

Acknowledgements: Cancer Research UK and EPSRC Cancer Imaging Centre, in association with the MRC and Department of Health (England) (C1060/A10334), NHS funding to the NIHR Biomedical Research Centre and The Royal Society.

References: [1] Schmid et al, IEEE Trans Med Imaging. 2006;25(12):1627-36, [2] Walker-Samuel et al, Magn Reson Med. 2009;62(2):420-429, [3] Kristoffersen, J Magn Reson Imaging. 2009;29(1):237-41.

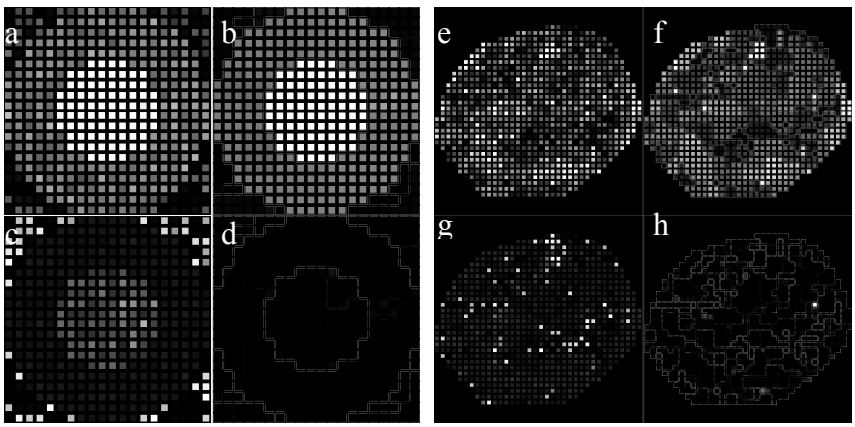

Figure 2: Simulated (left) and *in vivo* (right) ADC point estimates without adaptive smoothing (a and e) and with adaptive smoothing (b and f). ADC uncertainties with adaptive smoothing (c and g) and without adaptive smoothing (d and h). On all maps with adaptive smoothing, the borrowing strength is shown by a border around each pixel; bright lines indicate strong borrowing; dark lines indicate weak borrowing. Point estimates and uncertainty maps are windowed equivalently, illustrating the decrease in uncertainty when adaptive smoothing is implemented.